Available online at www.sciencedirect.com
ScienceDirect
Journal of the European Ceramic Society 27 (2007) 3469–3474
www.elsevier.com/locate/jeurceramsoc

Synthesis of $La_{0.9}Sr_{0.1}Ga_{0.8}Mg_{0.2}O_{2.85}$ by successive freeze-drying and self-ignition of a hydroxypropylmethyl cellulose solution

K. Traina [a,*], M.C. Steil [b,1], J.P. Pirard [c], C. Henrist [d], A. Rulmont [a], R. Cloots [a,d], B. Vertruyen [a]

[a] *Supratecs/LCIS, Chemistry Institute B6, University of Liège, Sart-Tilman, B-4000 Liège, Belgium*
[b] *UCCS, UMR CNRS 8181, ENSCL-ECL-USTL, Villeneuve d'Ascq Cedex, France*
[c] *Laboratoire de Génie Chimique, Chemistry Institute B6, University of Liège, B-4000 Liège, Belgium*
[d] *CATμ, Chemistry Institute B6, University of Liège, Sart-Tilman, B-4000 Liège, Belgium*

Received 12 September 2006; received in revised form 17 January 2007; accepted 27 January 2007
Available online 17 April 2007

Abstract

The present paper reports the synthesis of $La_{0.9}Sr_{0.1}Ga_{0.8}Mg_{0.2}O_{2.85}$ perovskite powders by a method combining freeze-drying and self-ignition of an aqueous solution of metallic nitrates containing hydroxypropylmethyl cellulose. The precursor powder obtained after self-ignition was submitted to various thermal treatments and the resulting powders were characterized by X-ray diffraction, electron microscopy, nitrogen adsorption–desorption isotherm analysis, mercury porosimetry and laser granulometry. It turns out that this synthesis method yields single-phase powders with good homogeneity and sinterability properties. The precursor powder treated at 1200 °C presents a coral-like structure which collapses under application of low uniaxial pressure, resulting in a narrow grain size distribution suitable for sintering (98.8% relative density for a pellet sintered at 1400 °C during 1 h). The fact that no milling step is necessary is an additional advantage of this method, which shows promising prospects for the synthesis of other multicationic oxides.

Keywords: Ionic conductor; Cryogel

1. Introduction

Since the discovery of oxygen conductivity in doped $LaGaO_3$ perovskites by Ishihara et al.,[1] these compounds have attracted much interest due to their potential application as electrolytes in solid oxide fuel cells (SOFC).[2–5] Since a solid state electrolyte must have a good chemical homogeneity with extremely low porosity, many authors have tried to improve the synthesis conditions of $La_{0.9}Sr_{0.1}Ga_{0.8}Mg_{0.2}O_{2.85}$ powders in order to achieve good sinterability. Solid state synthesis often results in the formation of secondary phases such as $LaSrGaO_4$, or $LaSrGa_3O_7$.[6–10] In order to improve the homogeneity, several wet chemistry methods were investigated by different authors (sol–gel synthesis,[7,11–13] gel method,[10,12,14–17] self-ignition synthesis[10,18–21]). Some of these techniques yield single-phase compounds. However, a milling step is usually needed in order to obtain a narrow grain size distribution in the micrometric or submicrometric range, as required for good sinterability properties.

The objective of the present study was to find a synthesis method to prepare pure powders with appropriate grain size distribution. That could be achieved by using a modified self-ignition technique. Self-ignition processes are characterized by the sudden release of gaseous decomposition products,[22] resulting in precursor powders with high specific surface area (leading to submicrometric particles at a later stage). However, the uncontrolled temperature increase during self-ignition frequently leads to the formation of intermediate phases. The chemical inhomogeneity introduced at that stage is often difficult to eliminate afterwards.[10,11,20,23–26] Therefore, on the one hand, it would be interesting to retain the properties of expansion resulting from the self-ignition process and on the other hand, to minimize the amount of combustible in order to keep the temperature as low as possible and to prevent the formation of secondary phases.

* Corresponding author. Tel.: +32 4 366 3532; fax: +32 4 366 3413.
E-mail address: karl.traina@ulg.ac.be (K. Traina).
[1] Laboratoire d'Electrochimie et de Physico-chimie des Matériaux et des Interfaces (LEPMI), CNRS, UJF, INPG, 1130 Rue de la Piscine, B.P. 75 38402 Saint Martin d'Hères Cedex, France.

0955-2219/$ – see front matter © 2007 Elsevier Ltd. All rights reserved.
doi:10.1016/j.jeurceramsoc.2007.01.017

These two requirements can be met by adding a suitable polymer to the cationic solution. First, the polymer increases the viscosity of the solution, so that it can be freeze-dried to form a dried material with a very open structure. Secondly, the polymer acts as combustible during the self-ignition of the freeze-dried material. Preliminary experiments showed that hydroxypropylmethyl cellulose (HPMC) induces appropriate viscosity at reasonably low concentration and is easily oxidized during self-ignition.[27] In the concentration range used for the synthesis, contamination of the final compound by sodium ions present in HPMC is very small (less than 0.2 wt%).

The present paper reports the synthesis of $La_{0.9}Sr_{0.1}Ga_{0.8}Mg_{0.2}O_{2.85}$ powder by successive freeze-drying and self-ignition of a HPMC solution. The precursor powder was submitted to various thermal treatments. The precursor and the calcined powders were characterized by different techniques in order to study their composition, crystallographic structure, microstructure, grain size distribution and sinterability.

2. Experimental section

2.1. Synthesis details

Polycrystalline $La_{0.9}Sr_{0.1}Ga_{0.8}Mg_{0.2}O_{2.85}$ was synthesized by a precursor method combining freeze-drying and self-ignition. Hereafter, the abbreviated formula LSGM12 is used for $La_{0.9}Sr_{0.1}Ga_{0.8}Mg_{0.2}O_{2.85}$; the numbers 1 and 2, respectively, mean substitution of 10% La by Sr and 20% Ga by Mg.

A 0.33 mol/l $Ga(NO_3)_3$ solution was prepared by dissolving metallic gallium (99.9% ABCR) with concentrated nitric acid. HNO_3 in excess was evaporated. The residue was dissolved in water and transferred into a volumetric flask. Stoichiometric amounts of $La(NO_3)_3{\cdot}6H_2O$ (99.9% REO, Alfa Aesar), $Sr(NO_3)_2$ (p.a. Acros) and $Mg(NO_3)_2{\cdot}6H_2O$ (p.a. Acros) were dissolved into 40 ml of the gallium nitrate solution. 4 g of hydroxypropylmethyl cellulose (Methocel® K4M, Colorcon) powder were dissolved in 160 ml water at 50 °C with magnetic stirring. The aqueous nitrate solution was then added at room temperature to the HPMC solution. After stirring during 2 min, the solution was placed in a refrigerator at −77 °C during 2 h before being freeze-dried during 72 h (Heto Drywinner DW 1.0–110).

The white freeze-dried material was then placed in an oven and heated under air at 3 °C/min from room temperature to 120 °C. During this cycle, it was observed that self-ignition usually occurred below 65 °C. After cooling to room temperature, the grey-brown precursor was powdered in a coffee grinder for a few seconds. In order to remove carbonaceous residues, the sample was then heated at 5 °C/min rate to 560 °C and kept at this temperature for 6 h. Finally, the resulting white-colored powder was calcined for 1 h at 700 °C, 1200 °C or 1400 °C with a 5 °C/min heating rate. After this calcination step, each sample was furnace cooled to room temperature. In order to investigate the sinterability of the powder obtained by this synthesis method, part of the powder calcined at 1200 °C was pelletized with 110 MPa uniaxial pressure. The pellets (1.5 mm thickness, 13 mm diameter) were sintered at 1400 °C for 1 h.

2.2. Characterizations

X-ray diffraction patterns were collected at room temperature with a Siemens D5000 powder diffractometer (Cu K_α radiation). Scanning electron microscopy (Philips ESEM XL30 FEG) was used to observe the morphology and particle size of powders and fractured surfaces. The cationic composition was investigated by Energy Dispersive X-ray analysis (EDAX Phoenix system coupled to the electron microscope). Specific surface area S_{BET} was determined from nitrogen adsorption–desorption isotherm analysis performed at 77 K using a Sorptomatic Carlo Erba 1900. Before nitrogen adsorption, the samples were outgassed for 12 h at room temperature and at 10^{-3} Pa pressure. The mercury porosimetry measurements were performed between 0.01 and 200 MPa after outgassing the sample for 2 h at room temperature and at 10^{-3} Pa pressure (Thermo Finnigan Pascal 140 between 0.01 and 0.1 MPa, Thermo Finnigan Pascal 240 between 0.1 and 200 MPa). The particle size distribution of powders was measured with a Malvern – Mastersizer 2000 – Hydro 2000S apparatus. The suspensions of powder in water were sonicated (Transsonic TS 540 Elma, 35 kHz – 77 W) before the particle size distribution measurements.

3. Results and discussion

The HPMC concentration and HPMC/nitrates ratio reported in the Section 2 were optimized during preliminary experiments using two criteria: (i) solution viscosity large enough to yield a sponge-like structure when freeze-dried and (ii) reproducible self-ignition. Additionally, it was found that the free-drying step is necessary in order to prevent the formation of separated gel and liquid phases when the HMPC-nitrates solution is heated to reach auto-ignition.

Self-ignition of the freeze-dried material resulted in an amorphous precursor compound, confirming that the oxidation of HPMC by nitrates does not lead to an excessive temperature increase. Fig. 1 presents XRD patterns collected on powders obtained by heating the precursor up to 560, 700, 1200 and 1400 °C. The product is still amorphous at 560 °C. At 700 °C,

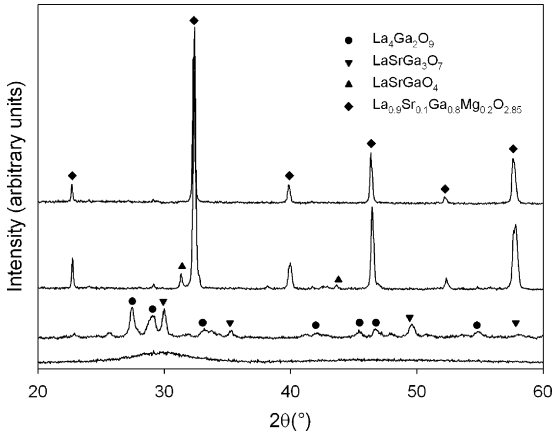

Fig. 1. XRD patterns collected on the powders obtained by heating the precursor up to (a) 560 °C, (b) 700 °C, (c) 1200 °C and (d) 1400 °C.

broad peaks corresponding to $La_4Ga_2O_9$ and $LaSrGa_3O_7$ phases can be observed. These intermediate phases frequently appear before the formation of the perovskite phase[8,12,18,20] and their elimination requires a thermal treatment at higher temperature. After a thermal treatment at 1200 °C, the XRD pattern shows that the powder contains a majority of LSGM12 perovskite phase, together with a small amount of $LaSrGaO_4$ secondary phase. The pattern of the powder heated up to 1400 °C corresponds to single phase LSGM12 and could be indexed in the *Imma* space group with cell parameters $a = 5.520$ Å, $b = 7.825$ Å and $c = 5.539$ Å, in good agreement with published data.[7]

Fig. 2 presents some electron micrographs of the powder at different stages of the synthesis route. The microstructure of the precursor is not significantly modified by the first treatment at 560 °C (see on Fig. 2a and b). The micrograph of the sample treated at 700 °C (Fig. 2c) highlights the nucleation of small grains of about 100–300 nm. This is consistent with the incipient crystallization observed by XRD. Fig. 2d shows the microstructure of the powder heated up to 1200 °C: grains between 500 nm and 1 μm are connected in a coral-like structure.

The specific surface area of the powder at different stages of the synthesis was measured by the BET technique.[29] The specific surface area of the precursor powder was found to be about 11.3 m^2/g. This value is higher than the results obtained for precursors prepared by Pechini technique (4.5 m^2/g),[12] sol–gel method (5.0 m^2/g)[12] or coprecipitation (8.0 m^2/g).[28] Huang and Goodenough[12] reported a much higher value (92 m^2/g) for a precursor prepared by hydrothermal synthesis but that precursor turned into an inhomogeneous compound after thermal treatment.

During the thermal cycle of the precursors studied in the present paper, the specific surface area S_{BET} increases from 11 m^2/g at 120 °C to 21 m^2/g at 560 °C, and then decreases to 7 m^2/g at 700 °C before reaching 1.5 m^2/g at 1200 °C. The increase of the specific surface area during the first stage of the thermal treatment is linked to the degradation of carbonaceous residues included in the mineral matrix and to the increase of the mesoporous volume (pores between 15 and 50 nm). The decrease of the specific surface area at higher temperature is linked to the formation and crystallization of the grains and simultaneously to the complete disappearance of the mesoporous volume caused by grain growth.

Mercury intrusion porosimetry is a powerful technique to follow powder sintering[29] because it makes it possible to investigate the porous structure of solid samples with pore sizes from a few microns down to about 4 nm.[30] In this method, mercury, which is a non-wetting liquid, is forced into the pores of a dry sample and the volume of mercury intruded into the pores is measured as a function of applied pressure. The analysis of mercury porosimetry data is based on the Washburn equation established in the case of cylindrical pores[31]:

$$r = -\frac{(2\gamma \cos\theta)}{P} \quad (1)$$

with γ the surface tension, θ the contact angle (in the range 130–140° for most materials) and P the pressure that must be applied to mercury to penetrate cylindrical pores of radius r. With $\gamma(\mathrm{Hg}) = 0.480$ N/m and $\theta = 140°$, the Washburn equation

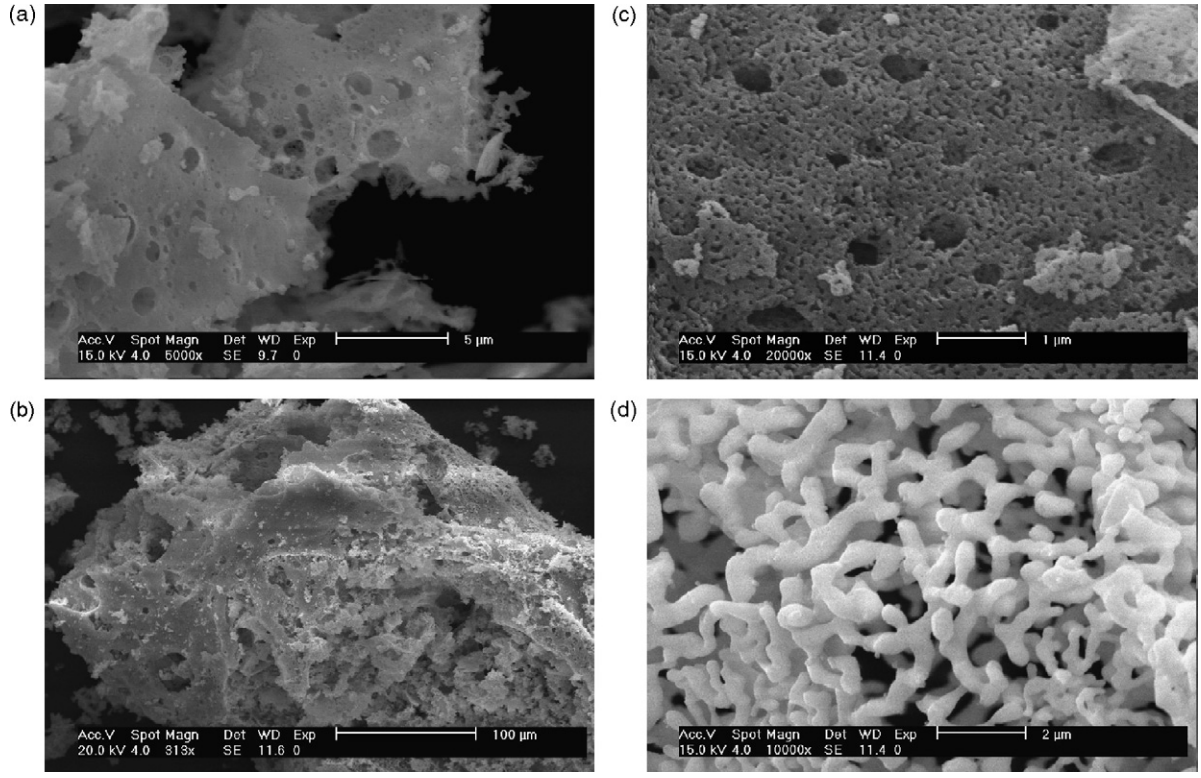

Fig. 2. Electron micrographs of the powders obtained (a) after self-ignition and after thermal treatment at (b) 560 °C, (c) 700 °C and (d) 1200 °C.

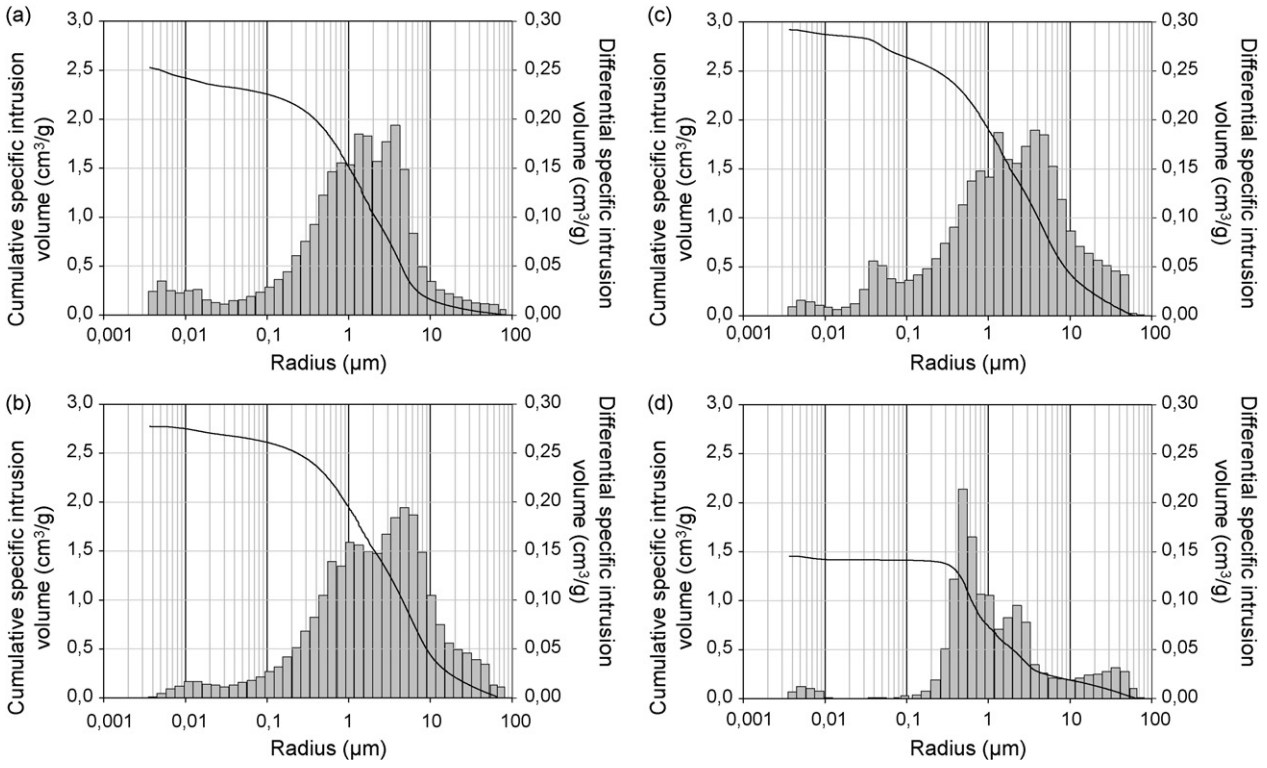

Fig. 3. Cumulative specific intrusion volume calculated with the Washburn equation (black line) and differential specific intrusion volume (histogram) of the powder obtained: (a) after self-ignition and after thermal treatment at (b) 560 °C, (c) 700 °C and (d) 1200 °C.

becomes:

$$r = \frac{0.7354}{P} \tag{2}$$

where P and r are expressed in MPa and μm, respectively.

Fig. 3 shows the results of mercury porosimetry measurements for the powder at different stages of the synthesis route. The differential (histogram) and cumulative (black line) specific intrusion volumes are plotted as a function of the pore radius calculated with Washburn's equation. Samples obtained after self-ignition (Fig. 3a) or after calcinations at 560 °C (Fig. 3b) or 700 °C (Fig. 3c) present mainly pore radius between 500 nm and 10 μm. In the case of the sample calcined at 700 °C (Fig. 3c), the differential specific intrusion volume histogram displays an additional peak centered on 40 nm. This value agrees well with the pore radius observed by electron microscopy (see Fig. 2c). Fig. 3d shows that calcination at 1200 °C leads to a significant decrease of the cumulative specific intrusion volume. This is due to the reduction of the macroporous volume resulting from the densification caused by grain growth and sintering. The differential specific intrusion volume histogram on Fig. 3d shows that the main peak is shifted to ∼600 nm. This result agrees with the pore size observed by scanning electron microscopy (see Fig. 2d). Thus, it seems that the classical cylindrical pore model is suitable to describe the texture of the powders synthesized by the freeze-drying/self-ignition method.

Mercury porosimetry results were used to evaluate the open porosity of the sample calcined at 1200 °C. The open porosity can be calculated by means of the equation:

$$\varepsilon = \frac{V_P}{(V_P + V_S)} \tag{3}$$

where ε, V_P and V_S are, respectively, the open porosity, the total open pore volume and the skeleton volume. The skeleton volume was calculated from the theoretical density ρ_S. Thus, for 1 g of powder, Eq. (3) becomes:

$$\varepsilon = \frac{V_P}{(V_P + 1/\rho_S)} \tag{4}$$

The total open pore volume V_P was determined from the mercury porosimetry measurements. The cumulative specific intrusion volume curve of the sample calcined at 1200 °C (see Fig. 3d) can be divided in three parts: (i) a first zone where the cumulative specific intrusion volume is almost constant (between 4 and 300 nm); (ii) a second zone where the cumulative specific intrusion volume varies strongly (between 300 nm and 3.7 μm) and (iii) a last zone where the variation is milder (above 3.7 μm). The cumulative specific intrusion volumes of the second and third zones are, respectively, considered as the volumes occupied by intragranular voids and intergranular voids. V_P in Eq. (4) is the cumulative specific intrusion volume corresponding to intragranular voids, obtained by subtracting the cumulative specific intrusion volumes at 300 nm and 3.7 μm. With $V_P = 1.17\ cm^3/g$ and $\rho_S = 6.67\ g/cm^3$ (PDF 01-070-2787) in Eq. (4), a value of 0.89 is obtained for the open porosity ε of the sample calcined at 1200 °C. This large value is consistent with the coral-like structure observed by electron microscopy (see Fig. 2d).

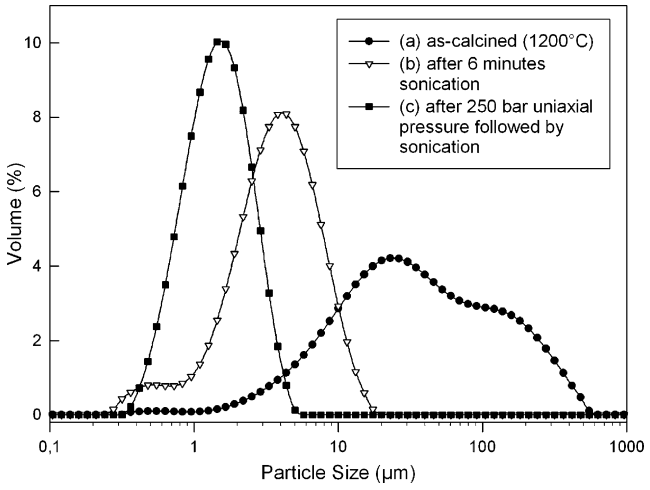

Fig. 4. Grain size distribution measured by laser granulometry on aqueous suspensions of the powder heated up to 1200 °C: (a) without any treatment, (b) after sonication and (c) after submitting the powder to 25 MPa uniaxial pressure (see text for more details).

The grain size distribution of the powders treated at 1200 °C or 1400 °C was studied by laser granulometry on aqueous suspensions. Data for the powder treated at 1200 °C are shown in Fig. 4. The as-calcined powder displays a very broad size distribution. After sonication for 6 min, the particle size distribution curve can be described as a main peak centered at ~3 μm ($d_{0.5}$ = 4 μm), with a tail in the <1 μm region. This means that sonication can break the largest agglomerates but that most of the "particles" are still larger than the size of the grains observed by electron microscopy. Therefore, the powder was pelletized with 25 MPa uniaxial pressure. The resulting pellet (thickness 0.5 mm, diameter 5 mm) was then dispersed into water by sonication for 30 s and the grain size distribution measurement was performed: the grain size distribution appears as a single peak, with $d_{0.1}$ = 0.8 μm, $d_{0.5}$ = 1.6 μm and $d_{0.9}$ = 3.0 μm. The homogeneous size distribution is confirmed by an electron micrograph of a green pellet fracture presented in Fig. 5: it turns out that the coral-like structure collapsed under pressure, resulting in individual grains. Qualitatively similar results were obtained for the sample treated at 1400 °C, whose size distribution curves are systematically shifted to slightly larger values.

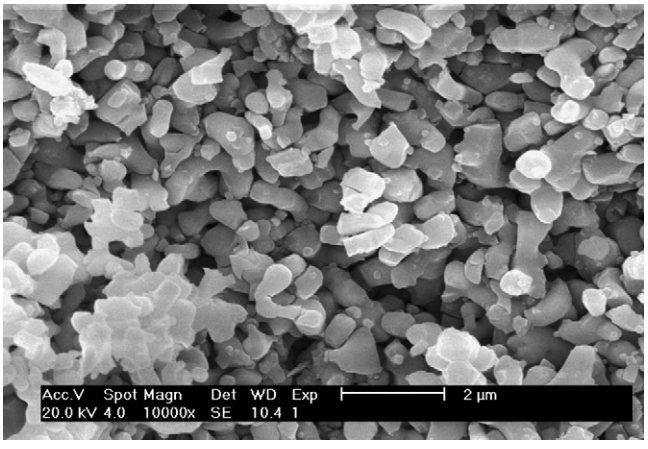

Fig. 5. Electron micrograph of a fractured pellet obtained by submitting the 1200 °C powder to 25 MPa uniaxial pressure.

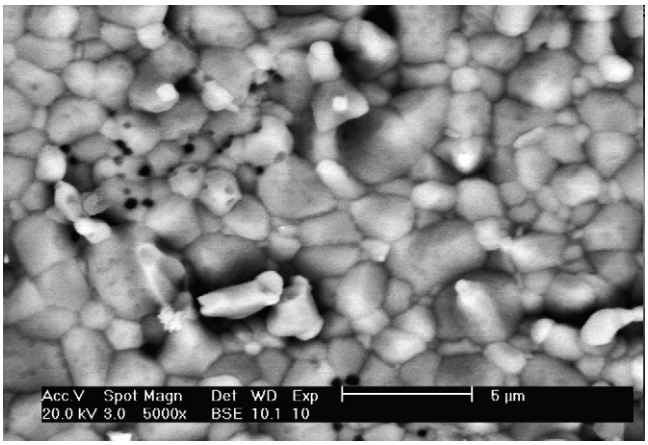

Fig. 6. Electron micrograph of a fracture in a pellet sintered at 1400 °C for 1 h.

In order to investigate the sinterability of the powder obtained by this synthesis method, some powder calcined at 1200 °C (i.e. with coral-like microstructure) was pelletized under 110 MPa uniaxial pressure and sintered at 1400 °C for 1 h. A representative microstructure of the fractured pellet is shown in Fig. 6. The density of the pellet, measured by Archimedes method, was 6.59 g/cm^3, which is close to the theoretical value 6.67 g/cm^3. X-ray diffraction showed that the $LaSrGaO_4$ peaks observed in the diffractogram at 1200 °C were no longer visible in the diffractogram collected on the pellet sintered at 1400 °C. The chemical homogeneity was ascertained by EDX analysis of a polished cross-section (see Fig. 7) through the pellet. No secondary phases were detected. Comparison of spectra collected in several zones confirmed the good cationic homogeneity of the material, with maximum deviations from the average values less than 0.5 mol%.

In summary, the characterization results have shown that the new method combining freeze-drying and self-ignition is suitable for the synthesis of LSGM12 powder with good homogeneity and sinterability properties.

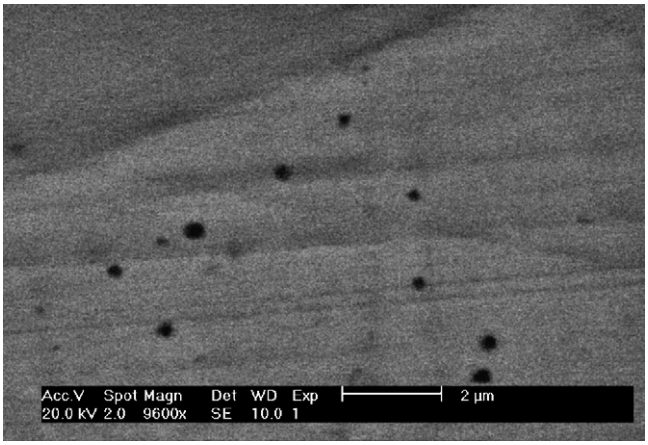

Fig. 7. Electron micrograph of a polished cross-section through a pellet sintered at 1400 °C for 1 h.

4. Conclusions

$La_{0.9}Sr_{0.1}Ga_{0.8}Mg_{0.2}O_{2.85}$ (LSGM12) powder was synthesized by a new method combining freeze-drying and self-ignition of an aqueous solution of metallic nitrates containing hydroxypropylmethyl cellulose. HPMC increased the viscosity of the solution, which could be freeze-dried to form a dry material with a very open structure. Then, the polymer played the role of combustible during the self-ignition of the freeze-dried material. This synthesis method yields single-phase LSGM12 powder with good homogeneity and sinterability properties, as required for potential application as electrolyte for solid oxide fuel cells. It turns out that the precursor powder treated at 1200 °C presents a coral-like structure. This structure presents a high porosity (0.89) which allows its easy collapse under application of low uniaxial pressure, resulting in a narrow grain size distribution ($d_{0.5} \sim 1.6\,\mu m$) suitable for sintering (98.8% relative density for a pellet sintered at 1400 °C during 1 h). An additional advantage of this method is that no milling step is necessary, preventing any contamination by grinding media. This combined freeze-drying/self-ignition technique shows promising prospects for the synthesis of other multicationic oxides.

Acknowledgments

This work was partially supported by the European Network of Excellence FAME and by the CGRI. B.V. thanks the FNRS (Belgium) for a "Postdoctoral researcher" fellowship.

References

1. Ishihara, T., Matsuda, H. and Takita, Y., Doped $LaGaO_3$ perovskite type oxide as a new oxide ionic conductor. *J. Am. Chem. Soc.*, 1994, **116**, 3801.
2. Feng, M. and Goodenough, J. B., A superior oxide-ion electrolyte. *Eur. J. Solid State Inorg. Chem.*, 1994, **31**, 663.
3. Huang, P.-N. and Petric, A., Superior oxygen ion conductivity of lanthanum gallate doped with strontium and magnesium. *J. Electrochem. Soc.*, 1996, **143**, 1644.
4. Kharton, V. V., Marques, F. M. B. and Atkinson, A., Transport properties of solid oxide electrolyte ceramics: a brief review. *Solid State Ionics*, 2004, **174**, 135–149.
5. Kim, J.-H. and Yoo, H.-I., Partial electronic conductivity and electrolytic domain of $La_{0.9}Sr_{0.1}Ga_{0.8}Mg_{0.2}O_{3-d}$. *Solid State Ionics*, 2001, **140**, 105–113.
6. Drennan, J., Zelizko, V., Hay, D., Ciacchi, F. T., Rajendran, S. and Badwal, S. P. S., Characterisation, conductivity and mechanical properties of the oxygen-ion conductor $La_{0.9}Sr_{0.1}Ga_{0.8}Mg_{0.2}O_{3-x}$. *J. Mater. Chem.*, 1997, **7**, 79.
7. Lerch, M., Boysen, H. and Hansen, T., High-temperature neutron scattering investigation of pure and doped lanthanum gallate. *J. Phys. Chem. Solids*, 2001, **62**, 445–455.
8. Huang, K., Tichy, R. S. and Goodenough, J. B., Superior perovskite oxide-ion conductor; strontium- and magnesium-doped $LaGaO_3$: I phase relationships and electrical properties. *J. Am. Ceram. Soc.*, 1998, **81**, 2565.
9. Azad, A. M. and Er, L. F., Microstructural evolution in B-site Mg-substitued $La_{0.9}Sr_{0.1}GaO_{3-d}$ oxide solid solution. *J. Alloys Compd.*, 2000, **306**, 103–112.
10. Majewski, P., Rozumek, M., Tas, A. C. and Aldinger, F., Processing of $(La,Sr)(Ga,Mg)O_3$ solid electrolyte. *J. Electroceram.*, 2002, **8**, 65.
11. Tao, S. W., Poulsen, F. W., Meng, G. Y. and Sorensen, O. T., High-temperature stability study of the oxygen-ion conductor $La_{0.9}Sr_{0.1}Ga_{0.8}Mg_{0.2}O_{3-x}$. *J. Mater. Chem.*, 2000, **10**, 1829.
12. Huang, K. and Goodenough, J. B., Wet chemical synthesis of Sr- and Mg-doped $LaGaO_3$ a perovskite-type oxide-ion conductor. *J. Solid State Chem.*, 1998, **136**, 274–283.
13. Huang, K., Feng, M. and Goodenough, J. B., Sol-gel synthesis of a new oxide-ion conductor Sr- and Mg-doped $LaGaO_3$ perovskite. *J. Am. Ceram. Soc.*, 1996, **79**, 1100.
14. Mathews, T., Sellar, J. R., Muddle, B. C. and Manoravi, P., Pulsed laser deposition of doped lanthanum gallate and in situ analysis by mass spectrometry of the laser ablation plume. *Chem. Mater.*, 2000, **12**, 917.
15. Tao, S. W., Wu, Q., Zhan, Z. and Meng, G. Y., Preparation of $LiMO_2$ (M = Co Ni) cathode materials for intermediate temperature fuel cells by sol-gel processes. *Solid State Ionics*, 1999, **124**, 53–59.
16. Schulz, O. and Martin, M., Preparation and characterisation of $La_{1-x}Sr_xGa_{1-y}Mg_yO_{3-(x+y)/2}$ for the investigation of cation diffusion processes. *Solid State Ionics*, 2000, **135**, 549–555.
17. Tas, A. C., Majewski, P. and Aldinger, F., Chemical preparation of pure and strontium- and/or magnesium-doped lanthanum gallate powders. *J. Am. Ceram. Soc.*, 2000, **83**, 2954.
18. Cong, L., He, T., Ji, Y., Guan, P., Huang, Y. and Su, W., Synthesis and characterization of IT-electrolyte with perovskite structure $La_{0.8}Sr_{0.2}Ga_{0.85}Mg_{0.15}O_{3-d}$ by glycine–nitrate combustion method. *J. Alloys Compd.*, 2003, **348**, 325–331.
19. Mathews, T. and Sellar, J. R., Observation of diffuse electron scattering in Sr- and Mg-doped $LaGaO_3$. *Solid State Ionics*, 2000, **135**, 411–417.
20. Tarancon, A., Dezanneau, G., Arbiol, J., Peiro, F. and Morante, J. R., Synthesis of nanocristalline materials for SOFC applications by acrylamide polymerisation. *J. Power Sources*, 2003, **118**, 256–264.
21. Stevenson, J. W., Armstrong, T. J., McCready, D. E., Pederson, L. R. and Weber, W. J., Processing electrical properties of alkaline earth-doped lanthanum gallate. *J. Electrochem. Soc.*, 1997, **144**, 3613.
22. Ganguli, D. and Chatterjee, M., *Ceramic Powder Preparation: A Handbook*. Kluwer, Boston, 1997.
23. Nguyen, T. L. and Dokiya, M., Electrical conductivity, thermal expansion and reaction of $(La,Sr)(Ga,Mg)O_3$ and $(La,Sr)AlO_3$ system. *Solid State Ionics*, 2000, **132**, 217–226.
24. Zheng, F., Bordia, R. K. and Pederson, L. R., Phase constitution in Sr and Mg doped $LaGaO_3$ system. *Mater. Res. Bull.*, 2004, **39**, 141.
25. Polini, R., Pamio, A. and Traversa, E., Effect of synthetic route on sintering behaviour, phase purity and conductivity of Sr- and Mg-doped $LaGaO_3$ perovskites. *J. Eur. Ceram. Soc.*, 2004, **24**, 1365–1370.
26. Stevenson, J. W., Armstrong, T. R., Pederson, L. R., Li, J., Lewinsohn, C. A. and Baskaran, S., Effect of A-site cation nonstoichiometry on the properties of doped lanthanum gallate. *Solid State Ionics*, 1998, **113–115**, 571–583.
27. Ziderman, I. I., Gregorski, K. S. and Friedman, M., Thermal analysis of protein-carbohydrate mixtures in oxygen. *Thermochim. Acta*, 1987, **114**, 109–114.
28. Du, Y. and Sammes, N. M., Fabrication of tubular electrolytes for solid oxide fuel cells using strontium- and magnesium-doped $LaGaO_3$ materials. *J. Eur. Ceram. Soc.*, 2001, **21**, 727–735.
29. Lecloux, A. J., Verleye, P., Bronckart, J., Noville, F., Marchot, P. and Pirard, J. P., Texture and sintering of zirconium dioxide-yttrium oxide ceramics. *React. Solids*, 1988, **4**, 309–325.
30. Lecloux, A. J., Texture of catalysts. In *Catalysis Science and Technology*, ed. J. R. Anderson and M. Boudart. Springer-Verlag, Berlin, 1981, pp. 171–230.
31. Washburn, E.W. The Dynamics of Capillary Flow. *Phys. Rev.*, 2nd Ser., 1921, **17**(3), 273–283.